was achieved during preparation of the sample by passing the host through a column heated to 150 °C packed with R-311 catalyst (Chemical Dynamics, Inc., South Plainfield, NJ).

The sample was deposited at the rate of 0.4 torr/min. All photochemical experiments unless otherwise indicated were carried out at 8 K. Gaseous samples ranged in M/R from 50 to 5000. The unlabeled thiadiazoles were prepared by standard methods.[60,61] The labeled thiadiazoles were prepared and characterized as previously described.[8d]

Photoirradiation of 1,2,3-Thiadiazole (5) in Solid Argon or Nitrogen. Initial experiments involved approximately a 5-min irradiation through a water filter, with the bare 100-W Hg lamp, which resulted in 70–90% destruction of the starting material (20–30 mm). The original infrared spectrum was replaced by a new spectrum with bands assigned to thioketene (15) at 3010 (w), 1755 (vs), and 692 cm^{-1} (m), and additional absorption including bands at 3315 (s), 2065 (vw), and 558 cm^{-1} that were assigned to ethynyl mercaptan 14. The bands of 14 and 15 grew at the same rate. Continued irradiation resulted in destruction of thioketene (15). Concurrent with the destruction of thioketene, a band appeared at 1520 cm^{-1} belonging to carbon disulfide. Photolysis of 1,2,3-thiadiazole 1a in a nitrogen matrix also gave 14 and 15 as products, but in a different ratio as judged by the relative intensities of bands. Preliminary experiments with deuterium-labeled species were carried out in a similar manner.

Photoirradiation of 1,2,3-Thiadiazole (5) in a Carbon Monoxide Matrix. 1,2,3-Thiadiazole (5) was mixed with carbon monoxide ($M/R \simeq$ 110, 16–38 mm) and deposited on the cesium iodide window at 20 K. Irradiation of matrix-isolated 5 to decomposition with Pyrex-filtered light also gave 14 and 15 as the major products. Within the limits of detectability of the Perkin-Elmer 521 spectrophotometer, neither bands due to carbonyl sulfide ($\nu = 2063$ cm^{-1}) nor the formyl radical ($\nu_3 = 1863$ cm^{-1}) were detected.

Photoirradiation of 1,2,3-Thiadiazole (5) in Acetylene-d_2 (28). 1,2,3-Thiadiazole 5 was mixed with acetylene-d_2 (28) ($M/R \simeq$ 200, 20 mm) and deposited at 50 K. Photolysis of 5 to decomposition with Pyrex-filtered light resulted in the formation of thioketene 15. There was no evidence for thioketene-d_2 ($\nu_{max} = 1735$ cm^{-1}, C=C str).

(61) Hurd, C. D.; Mori, R. I. *J. Am. Chem. Soc.* **1955**, *77*, 5359.
(62) Pacansky, J. *J. Phys. Chem.* **1977**, *81*, 2240.

Photoirradiation of 1,3,4-Thiadiazole (8) in an Argon Matrix. 1,3,4-Thiadiazole (8) was mixed with argon ($M/R \simeq$ 250 mm) and deposited on the CsI sample window which had been precooled to 20 K. Upon irradiation with a water-filtered mercury lamp light hydrogen cyanide dimer [$\nu_{max} = 3302, 2090$ cm^{-1} (w)] was observed as the major product.

General Procedure for Photolysis of ^{13}C-Labeled Thiadiazoles. Photolysis for 40 to 60 min of a matrix-isolated sample (40–50 mm) of isotopically labeled 1,2,3-thiadiazole in argon or nitrogen ($M/R \approx$ 500–1000) at 8 K with a 1000-W mercury–xenon lamp fitted with a 2500-Å interference filter resulted in loss of starting material and growth of bands belonging to thioketene, ethynyl mercaptan, and thiirene.

Initially ethynyl mercaptan and thioketene were formed directly from ^{13}C-labeled 1,2,3-thiadiazoles and maintained the integrity of the label (i.e., **31** was formed from **29**). If photolysis was carried out with Pyrex-filtered light, thiirene was not observed in the photolysate owing to its photoconversion to ethynyl mercaptans (**31** and **32**) and thioketenes (**33** and **34**). With 2500-Å light, thiirene is only slightly labile. Irradiation of thiirene using a 3500-Å interference filter resulted in its conversion to ethynyl mercaptan and thioketene. It was possible to selectively photolyze thiirene ($\lambda \sim 3500$ Å) in the presence of small quantities of **5**. The bands, assigned to labeled ethynyl mercaptans, thioketenes, and thiirenes that have been observed during the irradiation of labeled thiadiazoles, are listed in the tables.

Irradiation of Argon Matrix-Isolated Isothiazole (6) at 8 K. Photolysis of isothiazole (6) ($M/R \approx 400$) with light from a 1000-W mercury–xenon lamp fitted with a 2500-Å interference filter for 330-min led to destruction of the starting material and replacement of the starting infrared spectrum by bands assigned to thioketene (15) at $\nu_{max} = 3010$ (w), 1755 (vs), and 692 (s) cm^{-1}, ethynyl mercaptan (14) at $\nu_{max} = 3315$ (m) and 570 (m) cm^{-1}, thiirene (4) at $\nu_{max} = 3207, 3167, 3166, 1666, 914,$ and 572 cm^{-1}, and hydrogen cyanide at $\nu_{max} = 3303$ and 720 cm^{-1}. Further irradiation using a 3500-Å filter led to loss of bands due to **4**.

Kinetics and Thermodynamics for Ion-Molecule Association Reactions

J. S. Chang[‡] and D. M. Golden*

Department of Chemical Kinetics, SRI International, Menlo Park, California 94025. Received June 30, 1980

Abstract: Rate constants for ion-molecule association reactions have been calculated according to a simple model. The model, which mimics RRKM results, is constrained to reach limiting values corresponding to ADO (or Langevin) collision frequencies at the high-pressure limit and the strong-collison energy-transfer rate constant at the low-pressure limit. For those reactions at the low-pressure limit, the required information is the density of states (entropy) of the association complex. Low-pressure-limit rate constants and those in the "fall-off" regime are compared with data.

Introduction

Ion–molecule clustering or association reactions are of interest in physical, organic, and atmospheric chemistry. The overall process, typically written

$$A^+ + B + M \underset{k_r}{\overset{k_f}{\rightleftharpoons}} AB^+ + M \qquad (1)$$
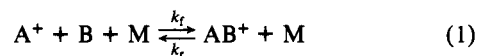
can more descriptively be illustrated as

$$A^+ + B \underset{k_b}{\overset{k_c}{\rightleftharpoons}} (AB^+)^* \xrightarrow{k_s[M]} AB^+ \qquad (2)$$
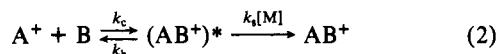
The collision rate constants, k_c and k_s, are given by Langevin[1]

and ADO theory[2-4] as appropriate.

It has already been pointed out[5,6] that this type of reaction is totally analogous to neutral radical-combination reactions. Thus, since it is really the microscopic reverse of a unimolecular bond-scission process, all the considerations associated with the

(1) G. Gioumousis and D. P. Stevenson, *J. Chem. Phys.*, **29**, 294 (1959).
(2) T. Su and M. T. Bowers, *J. Chem. Phys.*, **58**, 3027 (1973).
(3) T. Su and M. T. Bowers, *Int. J. Mass Spectrom. Ion Phys.*, **12**, 347 (1973).
(4) L. Bass, T. Su, W. J. Chesnavich, and M. T. Bowers, *Chem. Phys. Lett.*, **34**, 119 (1975).
(5) W. N. Olmstead, M. Lev-On, D. M. Golden, and J. I. Brauman, *J. Am. Chem. Soc.*, **99**, 992 (1977).
(6) (a) J. M. Jasinski, R. N. Rosenfeld, D. M. Golden, and J. I. Brauman, *J. Am. Chem. Soc.*, **101**, 2259 (1979); (b) D. R. Bates, *Proc. R. Soc. London, Ser. A*, **360**, 1 (1978); (c) E. Herbst, *J. Chem. Phys.*, **70**, 2201 (1979); (d) D. R. Bates, *ibid.*, **71**, 2318 (1979).

[‡]Postdoctoral research associate.

Table I. Low-Pressure-Limit Rate Constants[a]

| | reaction | k/cm^6 molecule^{-2} s^{-1} | | |
		calcd	exptl	ref
(1)	$H_3O^+ + H_2O + Ar \rightarrow H_3O \cdot H_2O^+ + Ar$	5 (−28)[b]	6 (−28)	18
			2 (−28)	19
	$H_3O^+ + H_2O + He \rightarrow H_3O \cdot H_2O^+ + He$	4 (−28)	6.7 (−28)	11
			7.2 (−28)	20
			1.2 (−27)	12
(2)	$NO^+ + CO_2 + N_2 \rightarrow NO^+CO_2 + N_2$	2 (−29)[c]	2.5 (−29)[c]	21
(3)	$O_2^+ + N_2O + N_2O \rightarrow O_2^+N_2O + N_2O$	3 (−29)[c]	5.2 (−29)[c]	22
(4)	$O_2^+ + O_2 + O_2 \rightarrow O_4^+ + O_2$	1.9 (−30)	2.5 (−30)	23a
			2.8 (−30)	23b
			2.4 (−30)	23c
(5)	$O_2^+ + N_2 + He \rightarrow O_2^+ \cdot N_2 + He$	1.5 (−29)[d]	1.9 (−29)[d]	22
		7 (−31)	8 (−31)	15
(6)	$O_2^+ + H_2O + O_2 \rightarrow O_2^+ \cdot H_2O + O_2$	1 (−28)	1 (−28)	24
			2.3 (−28)	25

[a] Calculations and experiments at 300 K unless otherwise cited. [b] Number in parentheses is the power of ten. [c] 200 K. [d] 80 K.

origin and nature of pressure dependence, as well as temperature dependence, arise when quantitatively discussing the rates of such processes. Ion-molecule association reactions are therefore treated by RRKM theory[5,6a] in order to codify and extrapolate the data to various conditions of temperature and pressure.

RRKM treatments involve complicated computer codes and detailed molecular information, and Troe and co-workers[7,8] have presented a model that allows a simpler calculation. We have adapted Troe's model to ion-molecule reactions, by taking into account the differences in the collision process.

Background

The model for the calculation of the association rate constant can be treated in three parts: high-pressure limit (second order), low-pressure limit (third order), and intermediate-pressure regime (fall-off region).

High-Pressure Limit. For the high-pressure-limit rate constant, we use Langevin and ADO theory to calculate k_c, the collision frequency between A^+ and B.

Low-Pressure Limit. We first calculate $(k_r)_0$, the low-pressure-limit rate constant in the unimolecular direction, for the decomposition of AB^+ (see eq 1). We then calculate the low-pressure-limit rate constant of interest from the overall equilibrium constant ($K = k_f/k_r$).

In complete analogy with Troe[7] we calculate the collision frequency between AB^+ and M by using ADO theory and a simple harmonic oscillator model followed by a few correction factors which account for (1) anharmonicity, (2) energy dependence of the density of states, (3) overall rotation, and (4) internal rotation, i.e.

$$k_r = \beta Z_{ADO} \frac{\rho_{vib,h}(E_0)kT}{Q_{vib}} \exp(-E_0/kT) F_{anh} F_E F_{rot} F_{int\ rot} \quad (3)$$

where β = collision efficiency (vida infra), Z_{ADO} = ADO collision frequency, $\rho_{vib,h}$ = harmonic oscillator density of states, Q_{vib} = vibrational partition function, and E_0 = critical energy (bond dissociation energy at 0/K). (Explicit formulas[7] for the various factors used in this calculation are listed in Appendix I.) Since one of the oscillators is represented by an R^{-4} potential, there may be a difference in anharmonicity correction factors between ion-molecule and neutral-molecule reactions, but the difference due to this one oscillator should be small, especially when the associated molecular ion has many atoms. β is assumed to be unity.[5] Equation 3 arises from[7]

$$\frac{(k_r)_0}{k_s[M]} = \frac{[AB^{+*}]}{[AB^+]} = \frac{Q_{AB^{+*}}}{Q_{AB^+}} = \frac{\int_{E_0}^{\infty} \rho(E)e^{-E/kT}\ dE}{Q_{AB^+}} = \frac{(k_r)_0}{\beta Z_{ADO}} \quad (4)$$

Table II. Collision Efficiences−Small Complex
$$O_2^+ + H_2O + M \rightarrow (O_2 \cdot H_2O)^+ + M$$

M	k_{exptl}[a]	ref
He	8.7×10^{-29}	24
	9×10^{-29}	25
Ar	1.7×10^{-28}	24
	2.0×10^{-28}	25
O_2	2.3×10^{-28}	24
	1×10^{-28}	25
N_2	2.5×10^{-28}	24
	2.8×10^{-28}	25

[a] cm^6 molecule^{-2} s^{-1}; 300 K. $k_{calcd} = 1 \times 10^{-28}$ cm^6 molecule^{-2} s^{-1} for all cases.

Note that this is independent of transition-state or RRKM theory.

This low-pressure-limit decompsition rate constant is then multiplied by the equilibrium constant to calculate the low-pressure-limit association rate constant. Unfortunately, thermochemical data are not always available. In these cases, we estimate some of the thermochemical data from geometry and vibrational frequencies to calculate the equilibrium constant.

Fall-Off Region. After we have obtained both the high-pressure-limit rate constant and the low-pressure-limit rate constant, the intermediate-pressure rate constant is obtained from a formula,[8] empirically designed to mimic RRKM curves, which has been successfully used[9,10] in neutral molecule association reactions. For each temperature, this formula is

$$k \simeq \frac{k_0[M]}{1 + k_0[M]/k_\infty} F_c^{\{1 + [\log(k_0[M]/k_\infty)]^2\}^{-1}} \quad (5)$$

where k_0 and k_∞ represent low-pressure-limit and high-pressure-limit rate constants, respectively.

F_c is a constant that can be evaluated[8] for different conditions. We find that for our limited purposes, a value of $F_c = 0.6$ is sufficient to reproduce values computed with a full RRKM calculation to within a factor of less than 2. (More accurate reproduction of RRKM can be obtained by using the more detailed formulas in ref 8.)

Results and Discussion

(A) Low-Pressure-Limit Association Rate Constants. The results of low-pressure-limit rate constant calculations for six association reactions are listed in Table I. The molecular parameters and thermochemical data used in the calculations are listed in Table IV. As shown in Table I, the agreement between the experimental data and the calculated rate constants is excellent. (This is also true for reactions shown in Tables II and III.) This not only means that this model works extremely well in relating the thermochemical and the kinetic data but also allows us to

(7) J. Troe, *J. Chem. Phys.*, **66**, 4758 (1977).
(8) K. Luther and J. Troe, "Proceedings of the 17th International Symposium on Combustion", Leeds, England, 1978, p 535.

(9) R. Zellner, *Ber. Bunsenges. Phys. Chem.*, **82**, 1172 (1978).
(10) D. M. Golden, J. S. Chang, and A. C. Baldwin, NASA Workshop on Stratospheric Chemistry. JPL Publication No. 79-27, Evaluation No. 2, April 15, 1979.

Table III. Collision Efficiencies–Large Complex
$$C_6H_6^+ + C_6H_6 + M \rightarrow (C_6H_6)_2^+ + M$$

M	$10^{25}k_{calcd}{}^a$	$k_{exptl}{}^a$	ref
He	3.8	4×10^{-27}	26
Ne	1.2	$\gtrsim 5 \times 10^{-28}$	26
Ar	1.3	7×10^{-27}	26
Kr	1	1.1×10^{-26}	28
Xe	1	1.6×10^{-26}	26
C_6H_6	2	1.2×10^{-25}	26

^{a} cm^6 molecule^{-2} s^{-1}; 300 K.

understand and predict many gas-phase ion-molecule association rate constants.

Of particular note is the inference that for some reactions that are difficult to study, we may predict rate constants if we have

the requisite thermochemical data. In fact, we argue[6a] that pursuit of the thermochemical information would be the more useful endeavor.

(B) Fall-Off Phenomena. Ion-molecule association rate constants will change from third order in the low-pressure regime to second order at the high-pressure limit. At the medium pressures where the transition takes place, "fall-off" phenomena are expected to be observed. RRKM treatments of this are adequate, as previously demonstrated.[5,6a] In this paper, we use eq 5 to predict the fall off. The result of this prediction is very close to an RRKM calculation which employs the same values of k_0 and k_∞.

A few experimental techniques have been widely used in studying the kinetics of ion-molecule association reactions. Most of them employ relatively low-pressure conditions such as the

Table IV. Vibrational Frequencies and Thermochemical Data

complex^a	freq	$\Delta H,^b \Delta S^c$	ref	complex^a	freq	$\Delta H,^b \Delta S^c$	ref
(I-1) $H_3O\cdot H_2O^+$	3100 (4)*	$\Delta H = -31.6$,	6a		1485 (2)		
	1800 (1)	$\Delta S = -24.6$			1326 (1)		
	1600 (2)				1310 (1)		
	500 (4)				1178 (2)		
410 (1)	410 (1)				1146 (1)		
	142 (2)				1089 (10)		
	50 (1)				1037 (2)		
(I-2) $NO^+\cdot CO_2$	1343	$\Delta H = -11.3$,	21		1010 (1)		
	667	$\Delta S = -25.0$					
	2349				992 (1)		
	2377				985 (1)		
					970 (2)		
	1600				847 (3)		
	500				800 (2)		
	100				703 (1)		
	100				600 (1)		
	500				400 (7)		
(I-3) $O_2^+\cdot N_2O$	1580	$\Delta H = -12.9$,	22		300 (2)		
	1275	$\Delta S = -29.0$	estimated		70 (5)		
	589 (2)				50 (1)		
	2225			(F) $CH_3NH_3\cdot CH_3NH_2^+$	3300 (4)	$\Delta H = -21.7$,	5
	1275				2970 (6)	$\Delta S = -23.6$	
	400				1600 (1)		
	100				1450 (6)		
	100				1175 (4)		
(I-4) O_4^+	1110	$\Delta H = -9.6$,	27, 23b		1000 (3)		
	1043	$\Delta S = -20.6$	27, 23b		900 (2)		
	800						
	400				820 (2)		
	400				740 (2)		
	100				600 (1)		
(I-5) $O_2^+\cdot N_2$	1100	$\Delta H = -7$,	22, 27		400 (1)		
	1100	$\Delta S = -20$			300 (2)		
	1200				200 (2)		
	400				175 (2)		
	400				100 (1)		
	75			(T) $C_2H_5ClCH_3^+$	3002	$\Delta H = -30.7$,	16
(I-6, II) $O_2^+\cdot H_2O$	1100	$\Delta H = -16$,	24, 25		580	$\Delta S = -30.7$	
	1043	$\Delta S = -17.9$			3184 (2)		
	3600				1383 (2)		
	3600				1020 (2)		
	400				1460 (1)		
	1000				1020 (2)		
	1000				1000 (1)		
	1400				1350 (1)		
	100				3000 (5)		
(III) $(C_6H_6)_2^+$	3082 (6)	$\Delta H = -15.1$,	6a		1150 (2)		
	3080 (2)	$\Delta S = -23.2$			400 (1)		
	3062 (1)				125 (2)		
	3060 (1)				100		
	3047 (2)				100		
	1597 (6)				550 (5)		
	1596 (2)						

^{a} I-1 through I-6 refer to Table I; II refers to Table II; III refers to Table III; F refers to the figure; T refers to the text. ^{b} ΔH for the reaction: $A^+ + B \rightarrow AB^+$ in kcal mol^{-1} (300 K). ^{c} ΔS for the reaction: $A^+ + B \rightarrow AB^+$ in cal mol^{-1} K^{-1} (300 K).
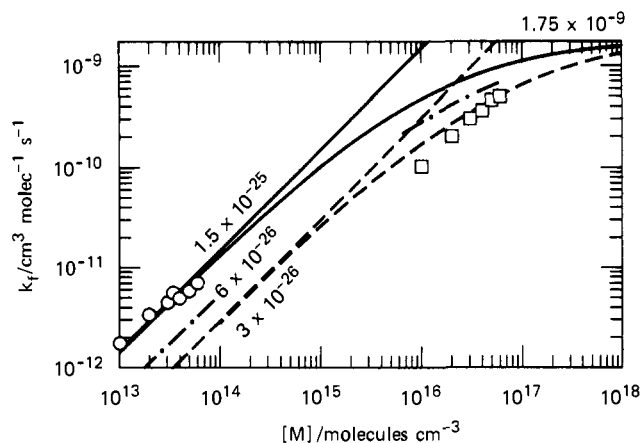
Figure 1. Pressure dependence of k_f at 300 K for the reaction CH_3NH_2 + $CH_3NH_3^+$ + M $\rightleftharpoons$ $CH_3NH_2-H^+NH_2CH_3$ + M (O, ref 13; □, ref 14): (—) a priori best estimates from methods outlined herein; (---) reduction of k_0 by a factor of 5 to accommodate data of ref 14; (-·-) compromise value to best accommodate high- and low-pressure data.

flowing-afterglow technique[11,12] and ion-cyclotron resonance spectroscopy at mili torr pressures, leading in general to near low-pressure-limit rate constants. However, some of the reactions may still show deviation from the low-pressure limit, particularly when mass spectrometric techniques in the torr range are employed. Extrapolation out of the experimental pressure range will be unreasonable[13] unless this is taken into account.

Prediction is compared to experiments using, as an example, the reaction

$$CH_3NH_3^+ + CH_3NH_2 + M \rightarrow CH_3NH_3^+CH_3NH_2 + M$$
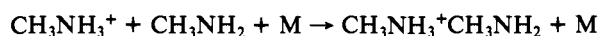
Two groups have studied this reaction by two different techniques. Neilson et al.[13] studied this reaction over the pressure range of 1×10^{-4} to 3×10^{-3} torr of CH_3NH_2 by using the ion-cyclotron resonance mass spectroscopic technique and concluded that the low-pressure-limit and high-pressure-limit rate constants were 1.8 $\times 10^{-25}$ cm^6 molecule^{-2} and 2.1 $\times 10^{-11}$ cm^3 molecule^{-1} s^{-1}, respectively.

Meot-Ner and Field[14] used a pulsed high-pressure mass spectrometer to study this reaction over the pressure range of 0.5–2 torr isobutane and concluded that the low-pressure-limit and high-pressure-limit rate constants were 2.5×10^{-26} cm^6 molecule^{-2} s^{-1} and 4.0×10^{-10} cm^3 molecule^{-1} s^{-1}.

The disagreement between these two reports results, in part, from systematic differences in the experiments and, in part, from an incorrect extrapolation of the data.[15] Figure 1 is illustrative. The higher pressure data[14] can be fit by assuming that $k_\infty = k_{ADO}$ = 1.75 $\times 10^{-9}$ cm^3 molecule^{-1} s^{-1} and $k_0 = 3 \times 10^{-26}$ cm^6 molecule^{-2} s^{-1}. We compute a value of $k_0 = 1.1 \times 10^{-25}$ cm^6 molecule^{-2} s^{-1} (in isobutane) by using the methods outlined herein. This is not out of the bounds of possible error. However, the lower pressure data[13] fit well the computed value (in methylamine) of $k_0 = 1.5 \times 10^{-25}$ cm^6 molecule^{-2} s^{-1}. Taking this latter at face value suggests that the higher pressure data are in error by a factor of ca. 2. Of course, a value of $k_0 = 6 \times 10^{-26}$ cm^6 molecule^{-2} s^{-1} splits the difference accommodating reasonable opposing errors in the two data sets, as well as an acceptable deviation from the calculation. (This latter line gives values within a factor of 2 of the RRKM calculations of Olmstead et al.,[5] who had only the high-pressure results at their disposal.)

Another example of the usefulness of this approach is illustrated for the reaction

$$C_2H_5^+ + CH_3Cl + CH_4 \rightarrow (C_2H_5ClCH_3)^+ + CH_4$$
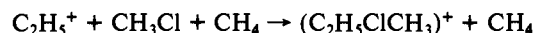
The rate constant for this process has been measured[16] at ~4 torr. The authors, having supposed the process to be in the low-pressure limit, interpreted the data to yield $k = 1.7 \times 10^{-26}$ cm^6 molecule^{-2} s^{-1} at 300 K. However, this rate constant multiplied by the pressure (i.e., 1.7×10^{-26} cm^6 molecule^{-2} s^{-1} $\times 1.3 \times 10^{17}$ molecule cm^{-3}) yields $k_f = 2.2 \times 10^{-9}$ cm^3 molecule^{-1} s^{-1}. The limiting values $(k_0$(cm^6 molecule^{-2} s^{-1}) = 3.5×10^{-25}, calculated by methods of ref 7; k_∞(cm^3 molecule^{-1} s^{-1}) = 2.02×10^{-9}, calculated from ADO theory along with eq 4) predict a value of k(cm^3 molecule^{-1} s^{-1}) = 1.8×10^{-9}, well within all the error limits. Notice that rather than following the author's supposition, at this pressure the process is very close to the high-pressure limit. This is to be expected for this large complex which is strongly bound (30.7 kcal mol^{-1}).

(C) M Effect (Nature of the Bath Gas). The assumption that β is unity (the strong collision assumption) has been discussed previously.[5] There is no reason to expect that the efficiency for the rare gases in not somewhat less than unity. We report here that for small ion-molecule complexes $(AB^+)^*$, $\beta = 1$ (this assumption is good within experimental scatter), but that for large $(AB^+)^*$ (see Table III), the efficiency of small bath gases seems to be low. These effects can be demonstrated with the following two reactions.

For small AB^+ molecules, the reaction

$$O_2^+ + H_2O + M \rightarrow O_2^+\cdot H_2O + M$$
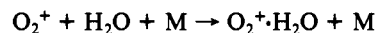
is used as an example. The M effect in the calculations resulted from the difference in Langevin collision frequencies which is proportional to $(\alpha_{M_1}\mu_{M_2}/\alpha_{M_2}\mu_{M_1})^{1/2}$ for different M, where α is polarizability and μ is the reduced mass of AB^+ and M. Usually, the calculated values of the rate constant for different M's are fairly close. The calculated and the experimental results are shown in Table II. All the experimental rate constants for different M's are within a factor of 3 compared with the calculated values, which lends credence to the notion that all bath gases are "good" third bodies.

For large AB^+ molecules, the reaction

$$C_6H_6^+ + C_6H_6 + M \rightarrow (C_6H_6)_2^+ + M$$

is used as an example. Table III shows all the experimental and calculated results. These results suggest that all rare gases are inefficient energy receivers or carriers, while C_6H_6 itself works well. This suggestion of inefficient energy transfer from a large ion-molecule complex to "small" bath-gas molecule warrants further investigation.

(D) Other Considerations. The temperature dependence of the rate constant can also be calculated according to this model. The results are similar to the results from RRKM calculations, which have also been shown to yield good agreement with some experiments.[5,6]

The uncertainties of around a factor of 2 or 3 in the low-pressure rate constant calculation are mainly due to current insufficient knowledge of the thermochemical data and of the geometry (structure) of the associated ion-molecule complex. For these association reactions, the influence on the rate constant from uncertainties in enthalpies is not as significant as those from entropies. This has been discussed previously with respect to both neutral and charged reactants.[6a,17] Therefore, it seems clear that any studies designed to yield entropic information on the ion-molecule complexes created by association reactions such as those dealt with herein will enhance the ability to predict rate constants for these processes.

(11) V. M. Bierbaum, M. F. Golde, and F. Kaufman, *J. Chem. Phys.*, **65**, 2715 (1976).

(12) C. J. Howard, V. M. Bierbaum, H. W. Rundle, and F. Kaufman, *J. Chem. Phys.*, **57**, 3491 (1972).

(13) P. V. Neilson, M. T. Bowers, M. Chau, W. R. Davidson, and D. H. Aue, *J. Am. Chem. Soc.*, **100**, 3649 (1978).

(14) M. Meot-Ner and F. H. Field, *J. Am. Chem. Soc.*, **97**, 5339 (1975).

(15) L. Bass, W. J. Chesnavich, and M. T. Bowers, *J. Am. Chem. Soc.*, **79**, 1501 (1979).

(16) D. K. Sharma and P. Kebarle, *J. Am. Chem. Soc.*, **100**, 5826 (1978).

(17) J. S. Chang, A. C. Baldwin, and D. M. Golden, *J. Chem. Phys.*, **71**, 2021 (1979).

(18) C. E. Young, D. Edelson, and W. F. Falconer, *J. Chem. Phys.*, **53**, 4295 (1970).

(19) U. A. Arifov, S. L. Pozharov, and I. G. Chemov., *Khim. Vys. Energ.*, **5**, 3 (1971); *Izv. Akad. Nauk. Uzb. SSR, Ser. Fiz.-Mat. Nauk.*, **15**, 49 (1971).

Conclusion

Thermal ion-molecule association reactions may be treated via RRKM theory[5,6,15] and thus also by the simplified computational schemes of Troe and co-workers[7,8] if neutral-neutral collision frequencies are replaced by ion-neutral frequencies (Langevin and ADO). Crucial inputs are the thermodynamic parameters of the association complex, especially the entropy.

Appendix I. List of Formulas

(a) ADO collision frequencies

$$Z_{ADO} = \frac{2\pi q}{\mu^{1/2}}\left[\alpha^{1/2} + C\mu_0\left(\frac{2}{\pi kT}\right)^{1/2}\right] \qquad (A1)$$

where q is the charge of the ion, μ is reduced mass between colliders, α is polarizability of the molecule, μ_0 is the dipole moment of the molecule, C is the correction factor as derived in ref 2, and k is the Boltzmann constant.

(b) Harmonic oscillator density of states

$$\rho_{vib,h} = [E + a(E)E_Z]^{s-1}/(s-1)!\prod_{i=1}^{s}(h\nu_i) \qquad (A2)$$

where E is the energy, E_Z is $\frac{1}{2}\sum_{i=1}^{s}h\nu_i$, s is number of oscillators, $a(E)$ is the empirical Whitten–Rabinovitch corrector, and ν_i are the vibrational frequencies.

(c) Anharmonicity correction factor

$$F_{anh} = \left(\frac{s-1}{s-\frac{3}{2}}\right)^{m} \qquad (A3)$$

where m is the number of oscillators that disappear during the dissociation reaction.

(d) Energy dependence of the density of states corrector is given as

$$F_E \simeq \sum_{v=0}^{s-1}\frac{(s-1)!}{(s-1-v)!}\left(\frac{kT}{E_0 + a(E_0)E_Z}\right)^{v} \qquad (A4)$$

(e) Rotational contribution

$$F_{rot} = [(s-1)!/(s+\tfrac{1}{2})!]\{[E_0 + a(E_0)E_Z/kT]\}^{3/2} \times$$
$$\left\{\frac{2.15(E_0/kT)}{2.15(E_0/kT)^{1/3} - 1 + [E_0 + a(E_0)E_Z/(s+\tfrac{1}{2})kT]}\right\} \qquad (A5)$$

(f) Internal rotation factor

$$F_{int\,rot} = \frac{(s-1)!}{(s-\tfrac{1}{2})!}\left(\frac{E_0 + aE_Z}{kT}\right)^{1/2}\left[1 - \exp\left(\frac{-E_0}{sV_0}\right)\right]\left\{\left[1 - \exp\left(\frac{-kT}{V_0}\right)\right]^{1.2} + \frac{\exp(-1.2kT/V_0)}{\sqrt{2\pi I_m kT/\hbar^2}[1 - \exp(-\sqrt{n^2\hbar^2 V_0/2I_m(kT)^2})]}\right\}^{-1} \qquad (A6)$$

(20) R. C. Bolden and N. D. Twiddy, *Discuss. Faraday Soc.*, **53**, 192 (1972).

(21) D. B. Dunkin, F. C. Fehsenfeld, A. L. Schmeltekopf, and E. E. Ferguson, *J. Chem. Phys.*, **54**, 3817 (1971).

(22) N. G. Adams, D. K. Bohme, D. B. Dunkin, F. C. Fehsenfeld, and E. E. Ferguson, *J. Chem. Phys.*, **52**, 3133 (1970).

(23) (a) J. D. Poyzant, A. J. Cunningham, and P. Kebarle, *J. Chem. Phys.*, **59**, 5615 (1973); (b) D. A. Durden, P. Kebarle, and A. Good, *ibid.*, **50**, 805 (1969); (c) A. Good, D. A. Durden, and P. Kebarle, *ibid.*, **52**, 222 (1970).

(24) C. J. Howard, V. M. Bierbaum, H. W. Rundle, and F. Kaufman, *J. Chem. Phys.*, **57.**, 57, 3491 (1972).

(25) F. C. Fehsenfeld, M. Moseman, and E. E. Ferguson, *J. Chem. Phys.*, **55**, 2115 (1971).

(26) V. G. Anicich and M. T. Bowers, *J. Am. Chem. Soc.*, **96**, 1279 (1974).

(27) G. S. Janik and D. C. Conway, *J. Phys. Chem.*, **71**, 823 (1967).

Protein Hydration from Water Oxygen-17 Magnetic Relaxation

Bertil Halle,[*†] **Thomas Andersson,**[‡] **Sture Forsén,**[‡] **and Björn Lindman**[†]

Contribution from Physical Chemistry 1 and Physical Chemistry 2, Chemical Center, S-220 07 Lund 7, Sweden. Received January 29, 1980

Abstract: Water oxygen-17 magnetic relaxation is shown to be a powerful technique for studying protein hydration. Longitudinal and transverse [17]O relaxation rates were measured at variable frequency (4–35 MHz), temperature, pH, and protein concentration in aqueous solutions of seven proteins. The data were analyzed in terms of a fast exchange two-state model with local anisotropy. A water [17]O quadrupole coupling constant of 6.67 MHz and an order parameter of 0.06 (from [17]O splittings in lyotropic liquid crystals) results in approximately two layers of hydration water having a reorientational rate less than 1 order of magnitude slower than that of bulk water. This rapid local motion has a small anisotropic component, which is averaged out by protein reorientation with a correlation time of the order of 10 ns. Due to electrostatic protein–protein interaction the protein reorientation is considerably slower than predicted by the Debye–Stokes–Einstein equation. Charged residues, particularly carboxylate, are more extensively hydrated than other residues, accounting for the variation in the extent of hydration between different proteins.

Introduction

Despite the multitude of experimental techniques that have been used to study protein hydration,[1-3] a consistent picture of the structural and dynamical details of the protein–water interaction has still not emerged. Thus, it is worthwhile to search for new

techniques to study the interacting water molecules as directly as possible.

To determine whether water [17]O magnetic relaxation is such a method, we have measured longitudinal and transverse [17]O

† Physical Chemistry 1.
‡ Physical Chemistry 2.

(1) Kuntz, I. D., Jr.; Kauzmann, W. *Adv. Protein Chem.* **1974**, *28*, 239.
(2) Eagland, D. In "Water-A Comprehensive Treatise"; Franks, F., Ed.; Plenum Press: New York, 1975; Vol. 4, Chapter 5.
(3) Berendsen, H. J. C. In "Water-A Comprehensive Treatise"; Franks, F.; Ed.; Plenum Press: New York, 1975; Vol. 5, Chapter 6.